Multi-mode mitigation in an optofluidic chip for particle manipulation and sensing

Philip Measor[1]*, Sergei Kühn[1], Evan J. Lunt[2], Brian S. Phillips[2], Aaron R. Hawkins[2], and Holger Schmidt[1]

[1]*School of Engineering, University of California Santa Cruz, 1156 High Street, Santa Cruz, CA, 95064, U.S.A.*
[2]*Department of Electrical and Computer Engineering, Brigham Young University, 459 Clyde Building, Provo, UT, 84602, U.S.A.*
**pmeasor@soe.ucsc.edu*

Abstract: A new waveguide design for an optofluidic chip is presented. It mitigates multi-mode behavior in solid and liquid-core waveguides by increasing fundamental mode coupling to 82% and 95%, respectively. Additionally, we demonstrate a six-fold improvement in lateral confinement of optically guided dielectric microparticles and double the detection efficiency of fluorescent particles.

OCIS codes: (220.2740) Geometric optical design; (230.7370) Waveguides; (230.1150) All-optical devices; (280.4788) Optical Sensing; (310.6845) Thin film devices and applications; (350.4855) Optical Manipulation.

References and links

1. D. Psaltis, S. R. Quake, and C. Yang, "Developing optofluidic technology through the fusion of microfluidics and optics," Nature **442**(7101), 381–386 (2006).
2. C. Monat, P. Domachuk, and B. Eggleton, "Integrated optofluidics: A new river of light," Nat. Photonics **1**(2), 106–114 (2007).
3. R. Bernini, S. Campopiano, L. Zeni, and P. M. Sarro, "ARROW optical waveguide based sensors," Sens. Actuators B Chem. **100**(1-2), 143–146 (2004).
4. H. Schmidt, and A. Hawkins, "Optofluidic waveguides: I. Concepts and implementations," Microfluidics and Nanofluidics **4**(1-2), 3–16 (2008).
5. A. Hawkins, and H. Schmidt, "Optofluidic waveguides: II. Fabrication and structures," Microfluidics and Nanofluidics **4**(1-2), 17–32 (2008).
6. D. Yin, J. P. Barber, A. R. Hawkins, and H. Schmidt, "Highly efficient fluorescence detection in picoliter volume liquid-core waveguides," Appl. Phys. Lett. **87**(21), 211111 (2005).
7. D. Yin, E. J. Lunt, M. I. Rudenko, D. W. Deamer, A. R. Hawkins, and H. Schmidt, "Planar optofluidic chip for single particle detection, manipulation, and analysis," Lab Chip **7**(9), 1171–1175 (2007).
8. P. Measor, S. Kühn, E. J. Lunt, B. S. Phillips, A. R. Hawkins, and H. Schmidt, "Hollow-core waveguide characterization by optically induced particle transport," Opt. Lett. **33**(7), 672–674 (2008).
9. M. I. Rudenko, S. Kühn, E. J. Lunt, D. W. Deamer, A. R. Hawkins, and H. Schmidt, "Ultrasensitive Qbeta phage analysis using fluorescence correlation spectroscopy on an optofluidic chip," Biosens. Bioelectron. **24**(11), 3258–3263 (2009).
10. S. Kühn, P. Measor, E. J. Lunt, B. S. Phillips, D. W. Deamer, A. R. Hawkins, and H. Schmidt, "Loss-based optical trap for on-chip particle analysis," Lab Chip **9**(15), 2212–2216 (2009).
11. A. W. Snyder, and J. D. Love, *Optical Waveguide Theory* (Springer, 1983).
12. R. Bernini, G. Testa, L. Zeni, and P. M. Sarro, "Integrated optofluidic Mach-Zehnder interferometer based on liquid core waveguides," Appl. Phys. Lett. **93**(1), 011106 (2008).
13. E. J. Lunt, P. Measor, B. S. Phillips, S. Kühn, H. Schmidt, and A. R. Hawkins, "Improving solid to hollow core transmission for integrated ARROW waveguides," Opt. Express **16**(25), 20981–20986 (2008).
14. J.-L. Archambault, R. Black, S. Lacroix, and J. Bures, "Loss calculations for antiresonant waveguides," J. Lightwave Technol. **11**(3), 416–423 (1993).
15. D. Marcuse, "Radiation losses of step-tapered channel waveguides," Appl. Opt. **19**(21), 3676–3681 (1980).
16. R. N. Thurston, E. Kapon, and A. Shahar, "Two-dimensional control of mode size in optical channel waveguides by lateral channel tapering," Opt. Lett. **16**(5), 306–308 (1991).
17. A. Ashkin, "Acceleration and trapping of particles by radiation pressure," Phys. Rev. Lett. **24**(4), 156–159 (1970).

#120356 - $15.00 USD Received 23 Nov 2009; accepted 9 Dec 2009; published 18 Dec 2009

Introduction

The field of optofluidics—the fusion of microfluidic environments and optical methods—has seen increasing interest in recent years [1,2]. One optofluidic biosensor approach has built upon antiresonant reflecting optical waveguide (ARROW) technology [3,4]. The platform was developed based on interconnected solid and liquid-core ARROWs using standard silicon microfabrication [4,5], and has demonstrated a device for compact, sensitive, and flexible particle sensing, transport, and trapping [6–10]. However, the dimensions of practical designs and the leaky waveguide nature of ARROWs [11], support multiple modes. The different propagation constants of the modes cause an unpredictable intensity beating along the waveguides, since the exact alignment to, and lengths of, the solid-core waveguides are unknown beforehand. Therefore, processes that rely on stable phase and intensity conditions can be disturbed. These include previous demonstrations of particle sensing/manipulation [6–10], as well as interferometric methods [12]. For these and many other applications, fundamental mode operation is desirable since it offers low loss propagation, small excitation volumes, and predictable mode field profiles. In this work, we present and experimentally demonstrate a design that optimizes the fundamental mode coupling of the optofluidic ARROW platform and discuss the impact on optical particle manipulation, trapping, and sensing applications.

First generation optofluidic platform

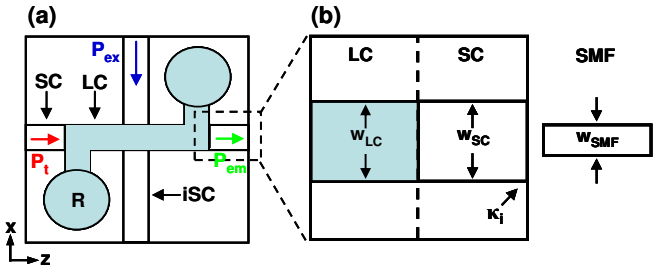

Fig. 1. (a) Top down schematic of an ARROW optofluidic platform with ridge-type solid-core ARROWs (SC), intersecting SC (iSC), liquid-core ARROWs (LC), and attached reservoirs (R). (b) Single-mode fiber (SMF), SC, to LC coupling scheme defining the SMF core width, w_{SMF}, SC width, w_{SC}, LC width, w_{LC}, and device facet input coupling coefficient, κ_i.

The optofluidic ARROW platforms used in this study consisted of specifically designed dielectric layers (three periods of SiN and SiO_2) providing optical isolation from the high index Si substrate. Layers surrounding a hollow core (LC, H_2O filled) are deposited (three periods of SiN and SiO_2) for low optical loss in a liquid core [4,5], and provide a microfluidic channel terminated by reservoirs (R). Ridge-type solid-core ARROWs (SC) are used for optical interfacing to single-mode fibers (SMF) and to define intersections (iSC) (Fig. 1). In this geometry, light may be used for optical manipulation (P_t), excitation of particles at the intersection (P_{ex}), and detection of particle fluorescence collected by the liquid-core waveguide (P_{em}).

As an example of the sensing capability in the ARROW platform, a solid and liquid-core waveguide width, w_{SC} and w_{LC} respectively, of 12μm was previously used to show single-particle sensitivity [7]. However, multiple modes are still excited in the solid-core ARROW with $w_{SC}>w_{SMF}$ [Fig. 1(b), typically w_{SC} = 12μm and w_{SMF} = 4μm], since there exists a significant overlap of the SMF TEM_{00} mode with the SC fundamental and higher order modes. The waveguide power input coupling coefficients for the SMF (mode 1) to SC (mode i) is defined as κ_i (for i = 1,2,3...). Since w_{SC} = w_{LC}, the fraction of power coupled to each mode from the solid-core to the liquid-core sections is approximately equal, but power loss can occur by fabrication-limited imperfections of the interface [13]. The theoretical coupling

#120356 - $15.00 USD Received 23 Nov 2009; accepted 9 Dec 2009; published 18 Dec 2009

coefficients reported throughout this paper were obtained using a commercial 2D finite element mode solver (FIMMWAVE, ©Photon Design). To measure the liquid core waveguide coupling, the x-z mode profile was obtained by filling the liquid core with aqueous fluorescent dye (rhodamine 6G, 1μM, in ultrapure water, 18MΩ-cm) and excited with frequency doubled Nd:YAG laser light (532 nm) via the SMF. The waveguide multimode beat pattern in the liquid core was observed with a charge-coupled device camera from above where the adjacent images are stitched together and normalized to reveal the long range trend [Fig. 2(a)]. The result shows excellent agreement with the corresponding simulated intensity profile [Fig. 2(b)] for w_{SMF} = 4μm, w_{SC} = w_{LC} = 12μm, and L_{SC} = 3.1mm with a beat length of $\Delta L = 2\pi/\Delta\beta \approx 359\mu m$ ($\Delta\beta = \beta_3 - \beta_1$ where β_i is the i^{th} mode propagation constant) and coupling coefficients of $\kappa_1 = 0.88$, $\kappa_2 = 0.02$, and $\kappa_3 = 0.08$.

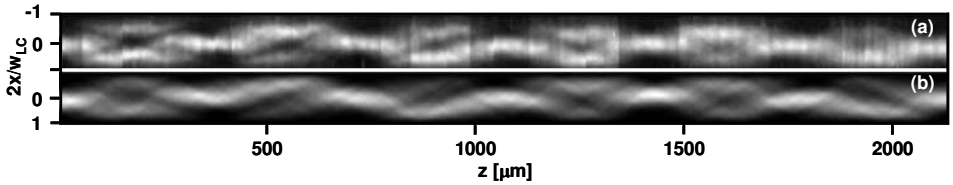

Fig. 2. First generation device liquid-core waveguide intensity pattern for (a) experimental measurement and (b) corresponding simulation.

Therefore, Fig. 2 reveals that even moderate coupling into higher-order modes in a liquid-core waveguide results in significant mode interference. To increase fundamental mode coupling, the solid-core waveguide parameters need to be optimized.

Second generation optofluidic platform

Typically, solid-core ARROW loss is limited by light scattering from the rough waveguide walls. As w_{SC} decreases or the mode order increases, the wall-field interaction is enhanced and the waveguide loss increases. Despite the larger waveguide loss, α, for narrow waveguides, the total device transmittance, T, may still increase for shorter lengths if κ_1 is large. Assuming $T_{wide,narrow} = \kappa_{wide,narrow}\exp(-\alpha_{wide,narrow}L_{SC})$, the length at which a wide waveguide has higher transmittance than a narrow waveguide is given by,

$$L_d = (\Delta\alpha)^{-1}\ln(\kappa^{-1}), \quad (1)$$

where Δα is the waveguide loss difference of the wide and narrow waveguide and κ is the ratio of coupling coefficients of the wide to narrow waveguide.

The simulated fundamental mode coupling from SMF to the solid-core waveguide as a function of w_{SC} is shown on Fig. 3(a) (w_{SMF} = 4μm), where a maximum at w_{SC} = 4μm is obtained. Solid-core waveguides with w_{SC} = 4μm were fabricated and the transmission as a function of solid-core length, L_{SC}, was measured [Fig. 3(b)]. A line was fitted to $\ln(T) = \ln(\kappa_1\kappa_o) - \alpha_{SC}L_{SC}$ to extract solid-core waveguide loss, α_{SC}, and $\kappa_1\kappa_o$, where κ_o is the solid-core waveguide output loss coefficient [Fig. 3(b)]. Assuming κ_o~0.96, due to the finite reflectance of the output facet, the measured fundamental mode input coupling efficiency is κ_1 = 0.82.

#120356 - $15.00 USD Received 23 Nov 2009; accepted 9 Dec 2009; published 18 Dec 2009

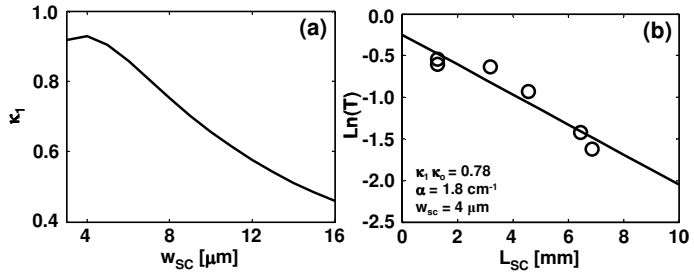

Fig. 3. Solid-core ARROW (a) fundamental mode coupling, κ_1, as a function of waveguide width, w_{SC} and (b) transmittance, T, as a function of waveguide length, L_{SC}.

Compared to the first generation platform with standard liquid-core ARROWs [13], the factor of 3 size reduction increased κ_1 and α_{SC} by a factor of 1.4 and 2.7, respectively. It can be seen that the measured κ_1 is lower than ideal, where the deviation is attributed to imperfect facets and alignment. Therefore, the L_{SC} needs to be no further than L_d~3mm (w_{SC} = 4μm) from the chip facet to yield a higher total transmittance. As in the first generation device, high solid to liquid-core waveguide coupling can be achieved by fabricating a device with w_{LC} = w_{SC}. However, $\alpha_{LC} \propto w_{LC}^{-3}$ [14], and thus a w_{LC} from 12 to 4μm will increase α_{LC} by a factor of 3^3.

One method to allow low α_{LC} and high κ_1, is to introduce a lateral taper [15,16]. This has the advantage of simultaneously achieving high κ_1 with a narrow ARROW and the low loss of the wide ARROW. The solid-core waveguide taper starts with the optimized w_{SC} = 4μm and gradually increases over a length, L_t, to w_{LC} thus matching the solid to liquid-core waveguide coupling perfectly (Fig. 4).

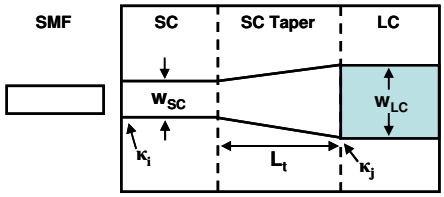

Fig. 4. Representation of the single-mode fiber (SMF) and solid-core ARROW (SC) interface coupling coefficient κ_i for SC width w_{SC}, SC taper over length L_t, and liquid-core ARROW (LC) coupling, κ_j for LC width w_{LC}.

As $L_t \to \infty$ the solid-core waveguide fundamental mode (mode 1) to liquid-core waveguide mode j = 1,2,3… coupling efficiency, κ_j, will tend toward unity [Fig. 4, 5(a)]. However, considering waveguide loss and device fabrication, a finite taper length of L_t = 550μm yields an optimal coupling of κ_1>0.99 [Fig. 5(a)].

#120356 - $15.00 USD Received 23 Nov 2009; accepted 9 Dec 2009; published 18 Dec 2009

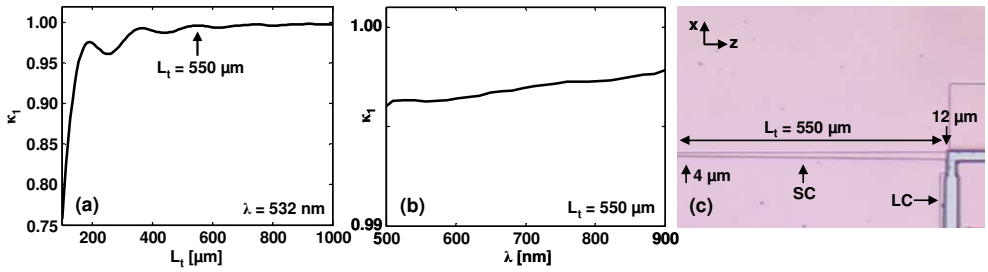

Fig. 5. Tapered solid-core ARROW (a) fundamental mode coupling coefficient, κ_1, and taper length, L_t, dependence; (b) κ_1 wavelength, λ, dependence for L_t = 550μm; and (c) fabricated device for w_{SC} = 4μm, w_{LC} = 12μm, and L_t = 550μm.

Figure 5(b) gives the wavelength dependence of κ_1 (L_t = 550μm) and shows the expected weak wavelength dependence allowing broadband operation. Figure 5(c) shows a section of the fabricated device with w_{SC} = 4μm, w_{LC} = 12μm, and L_t = 550μm. The second generation devices were standard liquid-core ARROWs and obtained (Fig. 6) using the same method as Fig. 2(a).

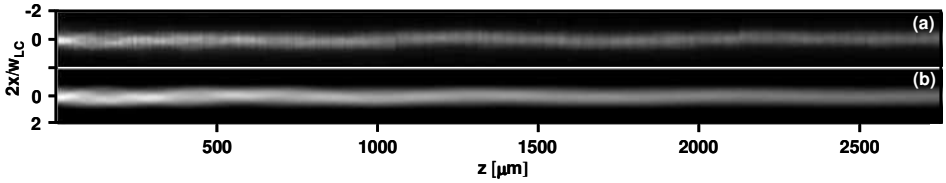

Fig. 6. Second generation device liquid-core ARROW intensity pattern for (a) experimental measurement and (b) corresponding simulation.

As can be seen in Fig. 6(a), the optimized device has virtually no intensity beating and again shows excellent agreement with simulations [Fig. 6(b)] for $w_{SMF} = w_{SC}$ = 4μm, w_{LC} = 12μm, and L_{SC} = 2.8μm with κ_1 = 0.95, κ_2 = 0.01, and κ_3 = 0.00. Therefore, the taper design successfully eliminates higher-order mode coupling.

Optical manipulation and sensing experiments

Now that the device supports a single mode, it can be used to center a particle in the waveguide channel via a guiding beam—a beam of light that uses the gradient force of radiation pressure to confine particles at the highest intensity [17]. Particle centering improves the fluorescence detection efficiency, since the overlap of the waveguide mode and fluorescent dipole emission profile is highest [6]. To demonstrate improved particle confinement, microspheres were introduced into the liquid core and manipulated with the guiding beam along z similar to [8]. First, the hollow-core waveguide was filled with ultra-pure water (18MΩ-cm) in one reservoir. Next, a suspension of 2μm diameter polystyrene particles (n~1.59 index at 532nm, Spherotech), ultra-pure water, and Triton X (0.03%) was introduced into the liquid core (0.4 particles/nL), via the opposite reservoir. A particle was then brought into the liquid core using pressure-induced flow. Once a microparticle is in the waveguide region, residual particle drift was balanced such that only Brownian motion was observed. Finally, the guiding beam was provided by a near infrared (NIR, λ = 820nm) beam coupled to the liquid-core waveguide via the taper (P_t~10-25mW). The microparticle trajectory (x-z) and lateral distribution, p(x), are shown in Fig. 7(a) for a particle under NIR irradiance (P_t~10mW).

#120356 - $15.00 USD Received 23 Nov 2009; accepted 9 Dec 2009; published 18 Dec 2009

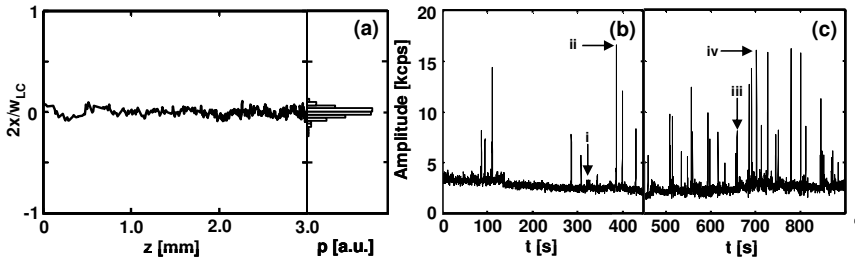

Fig. 7. (a) Particle trajectory in a liquid-core ARROW (left) and lateral position distribution, p(x), (right) with NIR beam guiding of a microparticle. The collected particle fluorescence with a guiding beam (b) off and (c) on.

As can be seen, the particle trajectory [Fig. 7(a)] is strongly confined to the center of the waveguide (x = 5.98 ± 0.23μm). This is a 6.2-fold improvement in the lateral standard deviation from the waveguide center over the first generation device [8].

To show that the combination of single-mode operation and optical confinement can be used to enhance the detection of particles, fluorescent microspheres (Invitrogen: 1μm diameter, λ_{ex} = 488nm, λ_{em} = 515nm, 1.2 particles/nL) were introduced into the liquid core and allowed to flow past the intersection using pressure driven flow. Fluorescence from particles traveling past the excitation region of the intersection (λ_{ex} = 488nm, P_{ex}~1μW) was collected by the liquid-core waveguide and detected (after filtering out the guiding and pump beams) via a single-photon avalanche photo diode [Fig. 7(b), 7(c)]. To visualize the particles, the intersection is monitored by a microscope system previously described [9]. While all the particles are visible in the microscope, their fluorescence is not coupled efficiently into the liquid-core waveguide if the particle is not centered inside the liquid core. It is seen under microscope observation that without a guiding beam, particles are freely diffusing in the x and y directions, as they flow along z, and the detection efficiency varies widely (Fig. 7i,ii). Many particles are not detected (Fig. 7i) if, for example, they reside next to the waveguide wall as shown in the still frame of Fig. 8(a) (for movies of extended observation see the supplementary material). However, when a guiding beam is used, the probability to find the particle in the center of the waveguide is increased and correspondingly the number of detected particles (Fig. 7iii,iv) substantially increases due to x and y centering [Fig. 7(c), 8(b)]. Note that adequate y centering is already achieved by careful choice of the vertical structure.

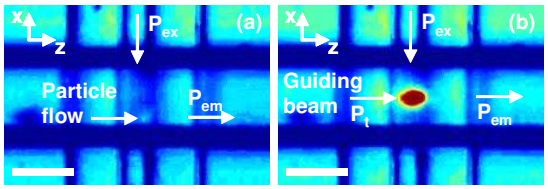

Fig. 8. Representative still frames of movies showing the fluorescence of particles as they flow past the intersection of the solid to liquid core ARROWs with a NIR guiding beam (a) off (Media 1) and (b) on (Media 2) (blue: low intensity and red: high intensity, scale bar ~12μm).

To detect a particle, we required a signal-to-noise ratio of 1:1 with respect to the background. The ratio of the number of detected particles to the number of particles that pass the intersection defines the detection efficiency, η. With a guiding beam, η increases from 41% to 85%. The undetected particles, with a guiding beam, are attributed to the confinement in the y-direction. Therefore, a single-mode guiding beam can be used to substantially increase the detection efficiency of a particle as it flows through an optofluidic channel.

#120356 - $15.00 USD Received 23 Nov 2009; accepted 9 Dec 2009; published 18 Dec 2009

Summary and conclusions

In summary, we have developed a new waveguide design for an ARROW-based optofluidic detection platform to improve optical interconnectivity and predictable field distribution. Fundamental mode operation was achieved despite the different working waveguide widths. This improvement was shown not only to benefit low-loss propagation but also for optical particle manipulation and detection. Specifically, the design resulted in a more than six-fold tighter microparticle lateral confinement and doubled the particle detection efficiency in fluorescence measurements. As a result, this device enables excellent all-optical particle manipulation control of fluorescence collection on an integrated optofluidic chip. Additionally, the platform enables future interferometric or optical manipulation devices that exploit the predictable mode profile and may be extended to tailor the field distribution at different points along the waveguide.

Acknowledgments

This work was supported by the NIH/NIBIB (R01EB006097, NIH-ARRA 1R21ER008802), NSF (ECS-0528730, ECS-0528714), and the W.M. Keck Center for Nanoscale Optofluidics at the University of California at Santa Cruz.

#120356 - $15.00 USD Received 23 Nov 2009; accepted 9 Dec 2009; published 18 Dec 2009